

# Negative Spin $\Delta_T$ noise Induced by Spin-Flip Scattering and Andreev Reflection

Sachiraj Mishra<sup>1,2,\*</sup> and Colin Benjamin<sup>1,2,†</sup>

<sup>1</sup>*School of Physical Sciences, National Institute of Science Education and Research, HBNI, Jatni-752050, India*

<sup>2</sup>*Homi Bhabha National Institute, Training School Complex, AnushaktiNagar, Mumbai, 400094, India*

We study charge  $\Delta_T$  noise, followed by an examination of spin  $\Delta_T$  noise, in the normal metal–spin flip–normal metal–insulator–superconductor (N–sf–N–I–S) junction. Our analysis reveals a key contrast: while charge  $\Delta_T$  noise remains strictly positive, spin  $\Delta_T$  noise undergoes a sign reversal from positive to negative, driven by the interplay between spin-flip scattering as well as Andreev reflection. In contrast, charge quantum shot noise remains positive and sign-definite, which is valid for spin quantum shot noise also. The emergence of negative spin  $\Delta_T$  noise has two major implications. First, it establishes a clear distinction between spin resolved  $\Delta_T$  noise and quantum shot noise: the former is dominated by opposite-spin correlations, whereas the latter is led by same-spin correlations. Second, it provides access to scattering mechanisms that are not captured by quantum shot noise alone. Thus, negative spin  $\Delta_T$  noise serves as a unique probe of the cooperative effects of Andreev reflection and spin flipping. We further place our results in context by comparing them with earlier reports of negative  $\Delta_T$  noise in strongly correlated systems, such as fractional quantum Hall states, and in multiterminal hybrid superconducting junctions. Overall, this work offers new insights into the mechanisms governing sign reversals in  $\Delta_T$  noise and highlights their role as distinctive fingerprints of spin-dependent scattering in superconducting hybrid devices.

## I. INTRODUCTION

The study of  $\Delta_T$  noise has recently attracted considerable attention from both theoretical [1–3] and experimental [4–6] researchers, due to its promise as an effective diagnostic probe in nonequilibrium quantum transport. This form of noise persists even when there is no net current, provided there is a finite temperature gradient across the system [1, 4, 7]. Experimentally,  $\Delta_T$  noise has been observed in a variety of platforms, including atomic-scale molecular junctions [4], mesoscopic quantum circuits [5], and metallic tunnel junctions [6]. Conceptually,  $\Delta_T$  noise represents a quantum contribution to shot noise driven solely by thermal gradients, offering a unique window into the nonequilibrium dynamics of charge and spin carriers in mesoscopic systems.

Recent advances have extended the study of  $\Delta_T$  noise to superconducting hybrid junctions, as demonstrated by several theoretical works [8–10]. In our recent study [10], we showed that charge  $\Delta_T$  noise together with spin  $\Delta_T$  noise can act as highly sensitive probes for identifying distinct categories of bound states in superconducting systems such as Yu–Shiba–Rusinov (YSR) bound states and Majorana bound states (MBS), thereby providing a diagnostic method that goes beyond conventional tunneling spectroscopy. While charge (spin)  $\Delta_T$  noise exhibits pronounced maxima or minima in regimes where Yu–Shiba–Rusinov states are present, no such signature is observed for MBS [10].

A recent study [2] on strongly correlated systems, specifically a two-terminal fractional quantum Hall setup with a quantum point contact, reported the emergence of negative charge  $\Delta_T$  noise. This counterintuitive behavior was attributed to the tunneling of fractionalized Laughlin quasiparticles between terminals, an effect absent when only electron tunneling is considered. Along similar lines, Ref.[11] linked the sign change in

$\Delta_T$  noise to the exchange statistics of tunneling quasiparticles, while Ref.[9] demonstrated a sign reversal in cross-correlated  $\Delta_T$  noise in a multiterminal superconducting–integer quantum Hall platform. In sharp contrast to these works, which rely on exotic strongly correlated quasiparticles and edge-mode transport, our study reveals that spin  $\Delta_T$  noise can undergo sign reversal purely from the synergy of spin-flip scattering as well as Andreev reflection in the ballistic regime of N–sf–N–I–S junction. This represents a fundamentally new finding: the first observation of negative spin  $\Delta_T$  noise without fractionalization or topological edge modes, offering a simpler and more experimentally accessible pathway to spin-resolved  $\Delta_T$  noise.

The structure of the paper is organized as: in Sec. II, we first present a brief overview of our chosen N–sf–N–I–S setup. We then explain the phenomena of spin-flip scattering by introducing a spin flipper at the metal/metal interface and an insulator at the metal–superconductor interface. Next, we discuss our results of charge  $\Delta_T$  noise, followed by spin  $\Delta_T$  noise, together with the corresponding charge as well as spin quantum shot noise in the considered setup. In Section IV, we present a comprehensive analysis of our findings, highlighting charge  $\Delta_T$  noise followed by spin  $\Delta_T$  noise, in comparison with the corresponding quantum shot noise. We also systematically compare our findings with previous studies [2, 9, 11] that reported negative charge  $\Delta_T$  noise. We conclude in Section V with a discussion on possible experimental realizations and a summary of our findings. The MATHEMATICA code used for calculating  $\Delta_T$  noise and quantum shot noise is available in Ref. [12].

## II. THEORY

In Fig. 1, a one-dimensional N–sf–N–I–S junction consisting of a spin magnetic impurity at the interface  $x = -a$  is shown. When an electron with spin either in up or down direction is incident from left normal metal  $N_1$  on the interfacial spin-flipper ( $x = -a$ ), there can be mutual spin-flip, and the electron may be normally reflected or Andreev reflected to normal

\* sachiraj29mishra@gmail.com

† colin.nano@gmail.com

metal  $N_1$  or transmitted to superconductor both as electron-like quasiparticle and hole-like quasiparticle. The BdG Hamiltonian describing the various scattering events occurring within the N-sf-N-I-S setup is written as

$$\mathcal{H} = \begin{pmatrix} (H_0(k) + H_{sf})\hat{I} & \hat{\Delta}(\mathbf{k})\Theta(x-a) \\ -\hat{\Delta}^*(-\mathbf{k})\Theta(x-a) & -(H_0^*(-k) + H_{sf}^*)\hat{I} \end{pmatrix}. \quad (1)$$

We consider the single-particle Hamiltonian  $H_0(k) = \hbar^2 q^2 / 2m^* + U\delta(x) - E_F$ , with  $q$  representing the wave vector,  $E_F$  the Fermi energy, and  $m^*$  the quasiparticle's effective mass. The term  $U\delta(x)$  models the insulating barrier through a delta-function potential. The effect of a localized magnetic impurity at the interface is incorporated via the spin-flip Hamiltonian  $H_{sf} = -J_0\delta(x)\vec{s} \cdot \vec{\Sigma}$ , with  $J_0$  quantifying the interaction strength linking the quasiparticle spin  $\vec{s}$  with the impurity spin  $\vec{\Sigma}$ . Regarding superconductivity, the pairing potential is  $\hat{\Delta}(\mathbf{k})$  (Refs. [13–15]). In the case of conventional  $s$ -wave singlet pairing, the gap takes the form  $\hat{\Delta}(\mathbf{k}) = i\Delta_0\chi_i$ , where  $\chi_i$  ( $i \in \{x, y, z\}$ ) denote the Pauli matrices. The exchange interaction present in  $H_{sf}$  is:

$$\vec{s} \cdot \vec{\Sigma} = s_z \cdot \Sigma_z + \frac{1}{2}(s^- \Sigma^+ + s^+ \Sigma^-). \quad (2)$$

The electron spin operators are denoted by  $s_x, s_y, s_z$ , whereas the spin-flipper (impurity) spin components are represented by  $\Sigma_x, \Sigma_y, \Sigma_z$ . The corresponding ladder operators are defined in

the usual way as  $s^\pm = s_x \pm is_y$  for the electron spin and  $\Sigma^\pm = \Sigma_x \pm i\Sigma_y$  for the spin-flipper spin.

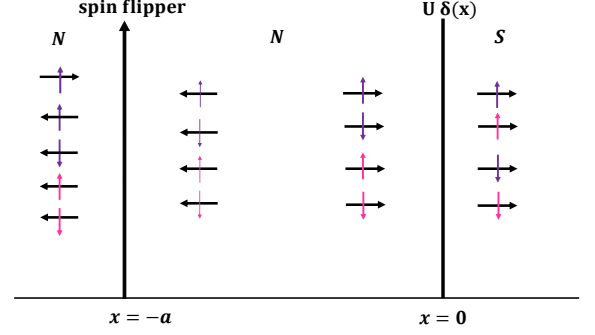


Figure 1: Schematic illustration of a one-dimensional N-sf-N-I-S junction, with a localized magnetic impurity situated at  $x = -a$  serves as a spin-flipper, and the insulating barrier at  $x = 0$  models the N-S interface. Purple  $\uparrow$  ( $\downarrow$ ) arrows represent spin-up (spin-down) electrons, whereas pink  $\uparrow$  ( $\downarrow$ ) arrows correspond to spin-up (spin-down) holes.

### A. Spin-flip scattering

The wave functions in all the three regions considered for spin-up electron incident from  $N_1$  can be written as (see, Fig. 1),

$$\begin{aligned} \phi_{N_1}(x) &= [e^{iq_e x} + b_{\uparrow\uparrow} e^{-iq_e x}] \Psi_m^s \chi_1 + b_{\downarrow\uparrow} e^{-iq_e x} \Psi_{m+1}^s \chi_2 + a_{\uparrow\uparrow} e^{iq_h x} \Psi_{m+1}^s \chi_3 + a_{\downarrow\uparrow} e^{iq_h x} \Psi_m^s \chi_4, \quad x < -a, \\ \phi_{N_2}(x) &= t_{\uparrow\uparrow} e^{iq_e x} \Psi_m^s \chi_1 + t_{\downarrow\uparrow} e^{iq_e x} \Psi_{m+1}^s \chi_2 + f_{\uparrow\uparrow} e^{-iq_e(x-a)} \Psi_m^s \chi_1 + f_{\downarrow\uparrow} e^{-iq_e(x-a)} \Psi_{m+1}^s \chi_2 \\ &\quad + g_{\uparrow\uparrow} e^{iq_h(x-a)} \Psi_{m+1}^s \chi_3 + g_{\downarrow\uparrow} e^{iq_h(x-a)} \Psi_m^s \chi_4 + h_{\uparrow\uparrow} e^{-iq_h x} \Psi_{m+1}^s \chi_3 + h_{\downarrow\uparrow} e^{-iq_h x} \Psi_m^s \chi_4, \quad -a < x < 0, \\ \phi_S(x) &= c_{\uparrow\uparrow} e^{ik_e x} \Psi_m^s \chi_1^S + c_{\downarrow\uparrow} e^{ik_e x} \Psi_{m+1}^s \chi_2^S + d_{\uparrow\uparrow} e^{-ik_h x} \Psi_{m+1}^s \chi_3^S + d_{\downarrow\uparrow} e^{-ik_h x} \Psi_m^s \chi_4^S, \quad x > 0. \end{aligned} \quad (3)$$

where  $\Psi_m^s$  is the eigenfunction of  $S_z$  such that  $S_z \Psi_m^s = m \Psi_m^s$ , with  $m$  being spin integer number and  $k_e$  being wave vector of electron, i.e.,  $k_e = \sqrt{\frac{2m^*}{\hbar^2}(E_F + \sqrt{E^2 - \Delta_0^2})} = k_F \sqrt{(1 + \frac{\sqrt{E^2 - \Delta_0^2}}{E_F})} \simeq k_F$  with energy of incident electron  $E > 0$ , and  $k_F = \sqrt{\frac{2m^* E_F}{\hbar^2}}$  is Fermi wave vector with  $E_F$  being the Fermi energy.  $\chi_i$  is the spinor in normal metal and  $\chi_i^S$  in superconductor. However, the superconducting gap  $\Delta$  changes with temperature, which is equal to  $\Delta(T) = \Delta_0 \sqrt{1 - \frac{T}{T_C}}$ , where  $\Delta_0 = 1.76 * k_B T_C$ , with  $T_C = 18K$  for  $Nb_3Sn$  [16, 17]. More details of the calculation is given in Ref. [10]. Reflection amplitudes for an incident spin-up electron to be reflected as spin-up electron is denoted as  $b_{\uparrow\uparrow}$  and to be reflected as spin-down electron is denoted as  $b_{\downarrow\uparrow}$ . Similarly,  $a_{\uparrow\uparrow}$  being the Andreev reflection amplitude with same spin, whereas  $a_{\downarrow\uparrow}$  being

the Andreev reflection amplitudes with different spins. In a similar manner,  $c_{\uparrow\uparrow}$  denotes the transmission coefficient corresponding to an incoming spin-up electron that propagates into the superconductor as a spin-up electron-like quasiparticle. On the other hand,  $c_{\downarrow\uparrow}$  represents the transmission amplitude for spin-up electron incident from the normal side to emerge as a spin-down electron-like quasiparticle. Likewise,  $d_{\uparrow\uparrow}$  and  $d_{\downarrow\uparrow}$  describe the conversion of the incoming electron into hole-like quasiparticles in the superconducting region, with  $d_{\uparrow\uparrow}$  corresponding to the same-spin process and  $d_{\downarrow\uparrow}$  corresponding to the opposite-spin process.

The electron spin is represented by the operator  $\vec{s}$ , while the spin-flipper's spin is denoted by  $\vec{\Sigma}$ . When these operators act on the spinor of an up-spin electron along with the spin-flipper

state, they yield the following relations [18–20]:

$$\vec{s} \cdot \vec{\Sigma} \begin{pmatrix} 1 \\ 0 \\ 0 \\ 0 \end{pmatrix} \Psi_m^s = \frac{m}{2} \begin{pmatrix} 1 \\ 0 \\ 0 \\ 0 \end{pmatrix} \Phi_m^s + \frac{\tau}{2} \begin{pmatrix} 0 \\ 1 \\ 0 \\ 0 \end{pmatrix} \Phi_{m+1}^s. \quad (4)$$

In this framework,  $\tau = \sqrt{(\Sigma - m)(\Sigma + m + 1)}$  and  $\tau_1 = \sqrt{(\Sigma + m)(\Sigma - m + 1)}$  correspond to the probabilities of spin flip for incident electrons having spin state up and down, respectively, from the left normal lead. Here,  $\Sigma$  stands for the spin-flipper's spin, while  $m$  takes integer values in the range  $-\Sigma, -\Sigma + 1, \dots, \Sigma - 1, \Sigma$ . Similarly, one can also see the similar equations involving the operation of  $\vec{s} \cdot \vec{\Sigma}$  on the spinor of spin-down electron, spin-up hole and spin-down hole, see Ref. [10].

The boundary matching conditions at the interfaces of the considered setup can be expressed as follows. At the position of the magnetic impurity,  $x = -a$ , we have

$$\begin{aligned} \phi_{N_1}(-a) &= \phi_{N_2}(-a), \\ \frac{d\phi_{N_2}(-a)}{dx} - \frac{d\phi_{N_1}(-a)}{dx} &= -\frac{2m^*J_0}{\hbar^2} (\vec{s} \cdot \vec{\Sigma}) \phi_{N_1}(-a), \end{aligned} \quad (5)$$

where the exchange interaction occurs due to the spin-flipper. At the normal metal–superconductor interface,  $x = 0$ , the boundary conditions are

$$\begin{aligned} \phi_{N_2}(0) &= \phi_S(0), \\ \frac{d\phi_S(0)}{dx} - \frac{d\phi_{N_2}(0)}{dx} &= \frac{2m^*U}{\hbar^2} \phi_{N_2}(0), \end{aligned} \quad (6)$$

where  $U$  denotes the strength of the insulating barrier. Substituting the wavefunctions defined in Eq. (3) into these boundary conditions allows us to solve for the scattering amplitudes corresponding to an incident electron with either spin orientation. In our calculations of quantum shot noise and  $\Delta_T$  noise, we use the dimensionless barrier strength  $Z = \frac{m^*U}{\hbar^2 k_F}$  and the dimensionless exchange interaction  $J = \frac{m^*J_0}{\hbar^2 k_F}$ .

1.  $\uparrow_{e-} \otimes \uparrow_S \xrightarrow{S=m} \frac{m}{2} (\uparrow_{e-} \otimes \uparrow_S)$
2.  $\uparrow_{e-} \otimes \downarrow_S \xrightarrow{S \neq m} \frac{m}{2} (\uparrow_{e-} \otimes \downarrow_S) + \frac{\tau}{2} (\downarrow_{e-} \otimes \uparrow_S)$
3.  $\downarrow_{e-} \otimes \uparrow_S \xrightarrow{S \neq -m} \frac{-m}{2} (\downarrow_{e-} \otimes \uparrow_S) + \frac{\tau_1}{2} (\uparrow_{e-} \otimes \downarrow_S)$
4.  $\downarrow_{e-} \otimes \downarrow_S \xrightarrow{S=-m} \frac{-m}{2} (\downarrow_{e-} \otimes \downarrow_S)$

Figure 2: Illustration of different spin configurations when spin  $\uparrow$  or  $\downarrow$  electron encounters a spin-flipper with  $S = \pm m$  or  $S \neq \pm m$ .  $\tau$  and  $\tau_1$  are spin-flip probabilities for spin-up and spin-down incident electrons.

One can also consider four different possible configurations as shown in Fig. 2. When the electron's elastic scattering time is much greater than the relaxation time of the spin-flipper  $\tau_e \gg \tau_{sf}$ , the spin-flipper will flip back before it interacts with

the upcoming incident electron, see Fig. 2. Therefore, spin magnetic moment  $m$  for a specific spin-flipper's spin  $S$  is not fixed, and to calculate any transport quantity, the average over all possible  $m$  values is taken. We consider the cases where a spin-up incident electron interacts in either spin-configuration 1 ( $S = m$ ) or spin-configuration 2 ( $S \neq m$ ). Likewise, for spin-down incident electron, the spin-flipper interacts via spin-configuration 3 ( $S \neq -m$ ) or spin-configuration 4 ( $S = -m$ ), as shown in Fig. 2.

In the following subsection, we compute the charge (spin) currents, along with the quantum charge (spin) quantum shot noise followed by  $\Delta_T$  noise, arising from spin-flip scattering in our setup depicted in Fig. 1.

## B. Charge and spin current

For the setup shown in Fig. 1, the average spin-polarized current can be expressed as [21, 22]

$$\langle I_i^s \rangle = \frac{2e}{h} \sum_{\substack{j,k \in \{1,2\} \\ \alpha, \beta, \gamma \in \{e,h\} \\ \sigma, \sigma' \in \{\uparrow, \downarrow\}}} \text{sgn}(\alpha) \int_{-\infty}^{\infty} dE \mathcal{M}_{jk;\beta\gamma}^{\sigma\sigma'}(i\alpha, s) \langle b_{j\beta}^{\sigma\dagger} b_{k\gamma}^{\sigma'} \rangle, \quad (7)$$

where  $\text{sgn}(\alpha) = +1$  ( $-1$ ) for electrons (holes). The matrix  $\mathcal{M}$  is defined as

$$\mathcal{M}_{jk;\beta\gamma}^{\sigma\sigma'}(i\alpha, s) = \delta_{ij} \delta_{ik} \delta_{\alpha\beta} \delta_{\alpha\gamma} \delta_{\sigma\sigma'} - S_{ij}^{\alpha\beta, \sigma\sigma'} S_{ik}^{\alpha\gamma, \sigma\sigma'}, \quad (8)$$

with  $i, j, k \in \{1, 2\}$  denoting the contacts (left normal lead and superconducting lead),  $\alpha, \beta, \gamma$  labeling electron and holes. Here,  $b_{j\beta}^{\sigma\dagger} b_{k\gamma}^{\sigma'}$  ( $b_{j\beta}^{\sigma\dagger} b_{k\gamma}^{\sigma'}$ ) is the creation (annihilation) operator for a particle of kind  $\beta$  ( $\gamma$ ) situated at contact  $j$  ( $k$ ) carrying spin  $\sigma$  ( $\sigma'$ ). The average value is given by  $\langle b_{j\beta}^{\sigma\dagger} b_{k\gamma}^{\sigma'} \rangle = \delta_{jk} \delta_{\beta\gamma} \delta_{\sigma\sigma'} f_{j\beta}(E)$ , where  $f_{j\beta}(E)$  is the Fermi distribution in contact  $j$  for particle  $\beta$ , independent of spin. Explicitly,  $f_{j\beta}(E) = \left[ 1 + \exp\left(\frac{E + \text{sgn}(\beta)eV_j}{k_B T_j}\right) \right]^{-1}$ , where  $\text{sgn}(\beta) = \pm 1$  for electrons (holes),  $k_B$  being Boltzmann constant with  $T_j$  denoting the temperature, whereas  $V_j$  is the voltage bias applied at lead  $j$ .

The mean charge current for  $N_1$  as shown in Fig. 1 can then be written as [18–20]

$$\langle I_1^c \rangle = \frac{2e}{h} \int_{-\infty}^{\infty} dE F^{ch}(E) (f_{1e}(E) - f_{2e}(E)), \quad (9)$$

with the function  $F^{ch}(E) = 1 + \mathcal{R}_{\uparrow\uparrow}^A + \mathcal{R}_{\downarrow\uparrow}^A - \mathcal{R}_{\uparrow\downarrow} - \mathcal{R}_{\downarrow\downarrow}$ . Here,  $\mathcal{R}_{\uparrow\uparrow}^A = |a_{\uparrow\uparrow}|^2$  is the Andreev reflection probability with same spin,  $\mathcal{R}_{\downarrow\uparrow}^A = |a_{\downarrow\uparrow}|^2$  is the Andreev reflection probability with opposite spin,  $\mathcal{R}_{\uparrow\uparrow} = |b_{\uparrow\uparrow}|^2$  is the normal reflection with same spin and  $\mathcal{R}_{\downarrow\uparrow} = |r_{\downarrow\uparrow}^{Na}|^2$  is the normal reflection with opposite spin. Similarly, mean spin current is given as

$$\langle I_1^s \rangle = \frac{2e}{h} \int_{-\infty}^{\infty} dE F^{sp}(E) (f_{1e}(E) - f_{2e}(E)), \quad (10)$$

with  $F^{sp}(E) = 1 + \mathcal{R}_{\uparrow\uparrow}^A - \mathcal{R}_{\downarrow\uparrow}^A - \mathcal{R}_{\uparrow\downarrow} + \mathcal{R}_{\downarrow\downarrow}$ . Since our setup preserves electron-hole symmetry, the currents (charge as well as spin) vanish when applied voltage bias is zero, even with a finite temperature gradient. This symmetry ensures that the Seebeck coefficient of the hybrid junction is identically zero, implying that the average current is solely governed by the applied voltage. Consequently, the average current becomes zero only when the voltage bias is zero.

### C. Quantum noise

Quantum noise autocorrelation implies the correlation of current fluctuations within  $N_1$  as shown in Fig. 1, and the formula for spin-polarised charge quantum noise correlation at zero frequency is

$$Q_{11}^{ch} = Q_{11}^{\uparrow\uparrow} + Q_{11}^{\uparrow\downarrow} + Q_{11}^{\downarrow\uparrow} + Q_{11}^{\downarrow\downarrow}. \quad (11)$$

Similarly, spin quantum noise is

$$Q_{11}^{sp} = Q_{11}^{\uparrow\uparrow} - Q_{11}^{\uparrow\downarrow} - Q_{11}^{\downarrow\uparrow} + Q_{11}^{\downarrow\downarrow}, \quad (12)$$

The spin polarized quantum noise valid at zero frequency in  $N_1$  is

$$Q_{11}^{ss'} = \sum_{\alpha, \beta \in \{e, h\}} Q_{11}^{ss', \alpha\beta} = \frac{e^2}{h} \int_{-\infty}^{\infty} dE \sum_{\sigma, \sigma' \in \{\uparrow, \downarrow\}} \sum_{\substack{j, k \in \{1, 2\} \\ \alpha, \beta, \gamma, \delta \in \{e, h\}}} \text{sgn}(\alpha) \text{sgn}(\beta) \mathcal{M}_{j\gamma, k\delta}^{\sigma\sigma'}(1\alpha, s) \mathcal{M}_{k\delta, j\gamma}^{\sigma'\sigma}(1\beta, s') f_{j\gamma}(E) [1 - f_{k\delta}(E)], \quad (13)$$

where  $\text{sgn}(\alpha) = +1$  ( $-1$ ) for electrons (holes). The matrix  $\mathcal{M}$  is defined as

$$\mathcal{M}_{j\gamma, k\delta}^{\sigma\sigma'}(p\alpha, s) = \delta_{pj} \delta_{pk} \delta_{\alpha\gamma} \delta_{\alpha\delta} \delta_{s\sigma} \delta_{s\sigma'} - s_{pj}^{\alpha\gamma, s\sigma} s_{pk}^{\alpha\delta, s\sigma'}. \quad (14)$$

The quantity  $s_{pk}^{\alpha\gamma, s\sigma}$  characterizes the amplitude representing a particle initially of type  $\gamma$  with spin index  $\sigma$  at terminal  $k$  to emerge at terminal  $p$  as particle of kind  $\alpha$  with spin  $s$ , where  $\gamma, \alpha \in e, h$  and  $\sigma, s \in \uparrow, \downarrow$ .

The complete expressions for  $Q_{11}^{ch}$  and  $Q_{11}^{sp}$  are provided in Ref. [10], where the Fermi wave vector parameter  $k_F a$  was fixed at  $0.85\pi$ . In contrast, in the present work we do not treat  $k_F a$  as a constant. Instead, we regard it as a variable that can change due to scattering events involving the spin flipper

as well as the insulating barrier. Consequently, in evaluating both the quantum shot noise (charge and spin) and the  $\Delta_T$  noise (charge and spin), we perform an average over  $k_F a$  by integrating the noise expressions from 0 to  $2\pi$  and dividing the result by  $2\pi$ . Therefore, the shot noise-like part of the total quantum noise  $Q_{11}^{sh; ss'}$  for  $s, s' \in \{\uparrow, \downarrow\}$ , which are given as,

$$\begin{aligned} Q_{11}^{sh; \uparrow\uparrow} &= Q_{11}^{sh; \downarrow\downarrow} = \frac{1}{2\pi} \int_0^{2\pi} d(k_F a) \left[ \frac{2e^2}{h} \int_{-\infty}^{\infty} dE (f_{1e} - f_{1h})^2 \left[ 2\mathcal{R}_{\uparrow\uparrow}^A \mathcal{R}_{\downarrow\uparrow} + 2\mathcal{R}_{\uparrow\uparrow}^A \mathcal{R}_{\uparrow\uparrow} + \mathcal{R}_{\uparrow\uparrow}^A \mathcal{R}_{\downarrow\uparrow} + \mathcal{R}_{\downarrow\uparrow}^A \mathcal{R}_{\uparrow\uparrow} - 2\text{Re}(a_{\downarrow\uparrow} b_{\uparrow\uparrow} a_{\uparrow\uparrow}^* b_{\downarrow\uparrow}^*) \right] \right. \\ &\quad \left. + \frac{2e^2}{h} \int_{-\infty}^{\infty} dE (f_{1e} - f_{2e})^2 \left[ (\mathcal{R}^A + \mathcal{R})(\mathcal{C}^S + \mathcal{D}^S) \right] \right], \\ Q_{11}^{sh; \uparrow\downarrow} &= Q_{11}^{sh; \downarrow\uparrow} = \frac{1}{2\pi} \int_0^{2\pi} d(k_F a) \left[ \frac{2e^2}{h} \int_{-\infty}^{\infty} dE (f_{1e} - f_{1h})^2 \left[ 4\text{Re}(a_{\uparrow\uparrow} b_{\uparrow\uparrow} a_{\downarrow\uparrow}^* b_{\uparrow\uparrow}^*) - \mathcal{R}_{\uparrow\uparrow}^A \mathcal{R}_{\downarrow\uparrow} - \mathcal{R}_{\downarrow\uparrow}^A \mathcal{R}_{\uparrow\uparrow} + 2\text{Re}(a_{\downarrow\uparrow} b_{\uparrow\uparrow} a_{\uparrow\uparrow}^* b_{\downarrow\uparrow}^*) \right] \right. \\ &\quad \left. + \frac{2e^2}{h} \int_{-\infty}^{\infty} dE (f_{1e} - f_{2e})^2 \left[ 4\kappa^2 \left( \text{Re}(c_{\uparrow\uparrow}^S c_{\downarrow\uparrow}^{S*}) + \text{Re}(d_{\uparrow\uparrow}^S d_{\downarrow\uparrow}^{S*}) \right) \times \left( \text{Re}(b_{\uparrow\uparrow} b_{\downarrow\uparrow}^*) + \text{Re}(a_{\uparrow\uparrow} a_{\downarrow\uparrow}^*) \right) \right. \right. \\ &\quad \left. \left. + 4\mathcal{R}_{\uparrow\uparrow}^A \mathcal{R}_{\downarrow\uparrow} + 4\mathcal{R}_{\downarrow\uparrow}^A \mathcal{R}_{\uparrow\uparrow} - 8\text{Re}(b_{\downarrow\uparrow} a_{\uparrow\uparrow}^* a_{\downarrow\uparrow} b_{\uparrow\uparrow}^*) \right] \right]. \end{aligned} \quad (15)$$

The scattering amplitudes for reflections within the first terminal are given by  $s_{11}^{ee; \uparrow\uparrow} = b_{\uparrow\uparrow}$ ,  $s_{11}^{ee; \downarrow\uparrow} = b_{\downarrow\uparrow}$ ,  $s_{11}^{he; \uparrow\uparrow} = a_{\uparrow\uparrow}$ , and

$s_{11}^{he; \downarrow\uparrow} = a_{\downarrow\uparrow}$ . For scattering from the superconducting terminal to  $N_1$ , we define  $\kappa = \sqrt{|u|^2 - |v|^2}$  to account for the supercon-



ducting coherence factors, and the corresponding amplitudes are expressed as  $s_{12}^{ee;\uparrow\uparrow} = \kappa c_{\uparrow\uparrow}^S$ ,  $s_{12}^{ee;\downarrow\uparrow} = \kappa c_{\downarrow\uparrow}^S$ ,  $s_{12}^{he;\uparrow\uparrow} = \kappa d_{\uparrow\uparrow}^S$ , and  $s_{12}^{he;\downarrow\uparrow} = \kappa d_{\downarrow\uparrow}^S$ . This notation compactly captures both the normal and Andreev scattering processes, with  $\kappa$  simplifying the expressions for transmission into the superconducting lead.

The quantities  $\mathcal{R}_{\uparrow\uparrow}^A$ ,  $\mathcal{R}_{\downarrow\uparrow}^A$ ,  $\mathcal{R}_{\uparrow\uparrow}$ , and  $\mathcal{R}_{\downarrow\uparrow}$  are defined immediately below Eq. (9). The transmission probabilities for electron-like quasiparticles entering  $N_1$  are expressed as  $C_S^{\uparrow\uparrow} = \kappa^2 |c_{\uparrow\uparrow}^S|^2$  for processes without spin flip and  $C_S^{\downarrow\uparrow} = \kappa^2 |c_{\downarrow\uparrow}^S|^2$  for spin-flip processes. Similarly, the corresponding transmission probabilities for hole-like quasiparticles returning from the su-

perconductor to the normal metal are given by  $\mathcal{D}_{\uparrow\uparrow}^S = \kappa^2 |d_{\uparrow\uparrow}^S|^2$  for no spin flip and  $\mathcal{D}_{\downarrow\uparrow}^S = \kappa^2 |d_{\downarrow\uparrow}^S|^2$  when a spin flip occurs. For brevity, we define the total Andreev reflection and normal reflection probabilities as  $\mathcal{R}^A = \mathcal{R}_{\uparrow\uparrow}^A + \mathcal{R}_{\downarrow\uparrow}^A$  and  $\mathcal{R} = \mathcal{R}_{\uparrow\uparrow} + \mathcal{R}_{\downarrow\uparrow}$ , and the total electron- and hole-like transmission probabilities as  $C^S = C_{\uparrow\uparrow}^S + C_{\downarrow\uparrow}^S$  and  $\mathcal{D}^S = \mathcal{D}_{\uparrow\uparrow}^S + \mathcal{D}_{\downarrow\uparrow}^S$ . The charge quantum shot noise is  $Q_{11}^{ch;sh} = Q_{11}^{sh;\uparrow\uparrow} + Q_{11}^{sh;\downarrow\uparrow} + Q_{11}^{sh;\downarrow\uparrow} + Q_{11}^{sh;\downarrow\downarrow}$ , and the spin quantum shot noise is  $Q_{11}^{sp;sh} = Q_{11}^{sh;\uparrow\uparrow} - Q_{11}^{sh;\uparrow\downarrow} - Q_{11}^{sh;\downarrow\uparrow} + Q_{11}^{sh;\downarrow\downarrow}$ .

The complete expressions for  $Q_{11}^{ch;sh}$  and  $Q_{11}^{sp;sh}$  follow directly from the above definitions.

$$\begin{aligned}
Q_{11}^{ch;sh} &= \frac{1}{2\pi} \int_0^{2\pi} d(k_F a) \left[ \frac{4e^2}{h} \int_{-\infty}^{\infty} dE \left\{ \left( 2\mathcal{R}_{\downarrow\uparrow}^A \mathcal{R}_{\downarrow\uparrow} + 2\mathcal{R}_{\uparrow\uparrow}^A \mathcal{R}_{\uparrow\uparrow} + 4\text{Re}(a_{\uparrow\uparrow} b_{\uparrow\uparrow}^* a_{\downarrow\uparrow}^* b_{\downarrow\uparrow}^*) \right) (f_{1e} - f_{1h})^2 \right. \right. \\
&\quad + \left( (\mathcal{R}^A + \mathcal{R})(C + \mathcal{D}) + 4\kappa^2 (\text{Re}(c_{\uparrow\uparrow}^S c_{\downarrow\uparrow}^{S*}) + \text{Re}(d_{\uparrow\uparrow}^S d_{\downarrow\uparrow}^{S*})) \right. \\
&\quad \times \left. \left. \left( \text{Re}(b_{\uparrow\uparrow} b_{\downarrow\uparrow}^*) + \text{Re}(a_{\uparrow\uparrow} a_{\downarrow\uparrow}^*) \right) + 4\mathcal{R}_{\uparrow\uparrow}^A \mathcal{R}_{\downarrow\uparrow} + 4\mathcal{R}_{\downarrow\uparrow}^A \mathcal{R}_{\uparrow\uparrow} - 8\text{Re}(b_{\downarrow\uparrow} b_{\uparrow\uparrow}^* a_{\downarrow\uparrow} a_{\uparrow\uparrow}^*) \right) (f_{1e} - f_{2e})^2 \right\} \right], \\
Q_{11}^{sp;sh} &= \frac{1}{2\pi} \int_0^{2\pi} d(k_F a) \left[ \frac{4e^2}{h} \int_{-\infty}^{\infty} dE \left\{ \left( 2\mathcal{R}^A \mathcal{R} - 8\text{Re}(a_{\uparrow\uparrow} a_{\downarrow\uparrow}^*) \text{Re}(b_{\uparrow\uparrow} b_{\downarrow\uparrow}^*) \right) (f_{1e} - f_{1h})^2 \right. \right. \\
&\quad + \left( (\mathcal{R}^A + \mathcal{R})(C^S + \mathcal{D}^S) - 4\kappa^2 (\text{Re}(c_{\uparrow\uparrow}^S c_{\downarrow\uparrow}^{S*}) + \text{Re}(d_{\uparrow\uparrow}^S d_{\downarrow\uparrow}^{S*})) \right. \\
&\quad \times \left. \left. \left( \text{Re}(b_{\uparrow\uparrow} b_{\downarrow\uparrow}^*) + \text{Re}(a_{\uparrow\uparrow} a_{\downarrow\uparrow}^*) \right) - \left( 4\mathcal{R}_{\uparrow\uparrow}^A \mathcal{R}_{\downarrow\uparrow} + 4\mathcal{R}_{\downarrow\uparrow}^A \mathcal{R}_{\uparrow\uparrow} - 8\text{Re}(b_{\downarrow\uparrow} a_{\uparrow\uparrow}^* a_{\downarrow\uparrow} b_{\uparrow\uparrow}^*) \right) \right) (f_{1e} - f_{2e})^2 \right\} \right].
\end{aligned} \tag{16}$$

At  $eV = 0$  with a temperature bias alone ( $T_1 - T_2 = \Delta T$ ) leads to the following relations between Fermi-Dirac distributions:  $f_{1e} = f_{1h}$  and  $f_{1e} \neq f_{2e}$ . Therefore, in the expressions of  $Q_{11}^{sh;\uparrow\uparrow}$ ,  $Q_{11}^{sh;\downarrow\uparrow}$ ,  $Q_{11}^{sh;\downarrow\uparrow}$  and  $Q_{11}^{sh;\downarrow\downarrow}$ , the terms with coefficient  $(f_{1e} - f_{1h})^2$  vanish and only terms with coefficient  $(f_{1e} - f_{2e})^2$  remain, which contribute to  $\Delta_T$  noise. Therefore, charge  $\Delta_T$  noise is given as  $\Delta_T^{ch} = \Delta_T^{\uparrow\uparrow} + \Delta_T^{\downarrow\uparrow} + \Delta_T^{\downarrow\uparrow} + \Delta_T^{\downarrow\downarrow}$  and spin  $\Delta_T$  noise is  $\Delta_T^{sp} = \Delta_T^{\uparrow\uparrow} - \Delta_T^{\downarrow\uparrow} - \Delta_T^{\downarrow\uparrow} + \Delta_T^{\downarrow\downarrow}$ , where

$$\begin{aligned}
\Delta_T^{\uparrow\uparrow} &= \Delta_T^{\downarrow\downarrow} = \frac{1}{2\pi} \int_0^{2\pi} d(k_F a) \left[ \frac{4e^2}{h} \int_{-\infty}^{\infty} dE (f_{1e} - f_{2e})^2 \right. \\
&\quad \times \left. \left[ (\mathcal{R}^A + \mathcal{R})(C^S + \mathcal{D}^S) \right] \right], \\
\Delta_T^{\downarrow\uparrow} &= \Delta_T^{\uparrow\downarrow} = \frac{1}{2\pi} \int_0^{2\pi} d(k_F a) \left[ \frac{4e^2}{h} \int_{-\infty}^{\infty} dE (f_{1e} - f_{2e})^2 \right. \\
&\quad \times \left[ 4\kappa^2 [\text{Re}(c_{\uparrow\uparrow}^S c_{\downarrow\uparrow}^{S*}) + \text{Re}(d_{\uparrow\uparrow}^S d_{\downarrow\uparrow}^{S*})] \right. \\
&\quad \times [\text{Re}(b_{\uparrow\uparrow} b_{\downarrow\uparrow}^*) + \text{Re}(a_{\uparrow\uparrow} a_{\downarrow\uparrow}^*)] \\
&\quad + 4\mathcal{R}_{\uparrow\uparrow}^A \mathcal{R}_{\downarrow\uparrow} + 4\mathcal{R}_{\downarrow\uparrow}^A \mathcal{R}_{\uparrow\uparrow} \\
&\quad \left. \left. - 8\text{Re}(b_{\downarrow\uparrow} a_{\uparrow\uparrow}^* a_{\downarrow\uparrow} b_{\uparrow\uparrow}^*) \right] \right].
\end{aligned} \tag{17}$$

Thus,  $\Delta_T^{ch}$  as well as  $\Delta_T^{sp}$  are given as

$$\begin{aligned}\Delta_T^{ch} &= \frac{1}{2\pi} \int_0^{2\pi} d(k_F a) \left[ \frac{4e^2}{h} \int_{-\infty}^{\infty} dE (f_{1e} - f_{2e})^2 \left[ (\mathcal{R}^A + \mathcal{R})(C^S + \mathcal{D}^S) + 4\kappa^2 \left( \text{Re}(c_{\uparrow\uparrow}^S c_{\downarrow\uparrow}^{S*}) + \text{Re}(d_{\uparrow\uparrow}^S d_{\downarrow\uparrow}^{S*}) \right) \right. \right. \\ &\quad \times \left( \text{Re}(b_{\uparrow\uparrow} b_{\downarrow\uparrow}^*) + \text{Re}(a_{\uparrow\uparrow} a_{\downarrow\uparrow}^*) \right) \\ &\quad \left. \left. + 4\mathcal{R}_{\uparrow\uparrow}^A \mathcal{R}_{\downarrow\uparrow} + 4\mathcal{R}_{\downarrow\uparrow}^A \mathcal{R}_{\uparrow\uparrow} - 8 \text{Re}(b_{\downarrow\uparrow} a_{\uparrow\uparrow}^* a_{\downarrow\uparrow} b_{\uparrow\uparrow}^*) \right] \right], \\ \Delta_T^{sp} &= \frac{1}{2\pi} \int_0^{2\pi} d(k_F a) \left[ \frac{4e^2}{h} \int_{-\infty}^{\infty} dE (f_{1e} - f_{2e})^2 \left[ (\mathcal{R}^A + \mathcal{R})(C^S + \mathcal{D}^S) - 4\kappa^2 \left( \text{Re}(c_{\uparrow\uparrow}^S c_{\downarrow\uparrow}^{S*}) + \text{Re}(d_{\uparrow\uparrow}^S d_{\downarrow\uparrow}^{S*}) \right) \right. \right. \\ &\quad \times \left( \text{Re}(b_{\uparrow\uparrow} b_{\downarrow\uparrow}^*) + \text{Re}(a_{\uparrow\uparrow} a_{\downarrow\uparrow}^*) \right) \\ &\quad \left. \left. - \left( 4\mathcal{R}_{\uparrow\uparrow}^A \mathcal{R}_{\downarrow\uparrow} + 4\mathcal{R}_{\downarrow\uparrow}^A \mathcal{R}_{\uparrow\uparrow} - 8 \text{Re}(b_{\downarrow\uparrow} a_{\uparrow\uparrow}^* a_{\downarrow\uparrow} b_{\uparrow\uparrow}^*) \right) \right] \right].\end{aligned}\quad (18)$$

Eqs. (16) and (18) are the central formulae of the paper and we further use them for the results and analysis.

### III. RESULTS AND DISCUSSION

This section presents an analysis of charge followed by spin  $\Delta_T$  noise in the considered junction. We further examine quantum shot noise (both charge as well as spin) in the same setup.

#### A. Charge & spin $\Delta_T$ noise

To evaluate and interpret the charge as well as spin components of the  $\Delta_T$  noise—denoted by  $\Delta_T^{ch}$  and  $\Delta_T^{sp}$ , respectively, we apply zero voltage bias, subject to a finite thermal gradient. The temperatures of the two leads are set as  $T_1 = T + \Delta T/2$ ,  $T_2 = T - \Delta T/2$ , where  $T$  is the average temperature and  $\Delta T$  the applied temperature difference. In Fig. 3, we plot  $\Delta_T^{ch}$  and  $\Delta_T^{sp}$  as functions of strength of the barrier of the spin-flipper ( $J$ ), the strength of the barrier of the impurity ( $Z$ ), and the normalized temperature ( $\frac{T}{T_C}$ ). An important observation:  $\Delta_T^{ch}$  remains strictly positive throughout the entire parameter space and also at elevated temperatures where quasiparticle tunneling becomes significant and tends to compete with Andreev reflection processes. This is clearly visible in Fig. 3(a), where  $\Delta_T^{ch}$  shows no sign change for any combination of  $J$ ,  $Z$ , and  $\frac{T}{T_C}$ . On the other hand,  $\Delta_T^{sp}$  reveals a richer and more intricate behavior, strongly influenced by the interplay between spin-flip scattering, Andreev processes, and quasiparticle transport. At low temperatures,  $\Delta_T^{sp}$  is consistently negative across the full range of  $J$  and  $Z$  values (see, Fig. 3(b)). This negativity  $\Delta_T^{sp}$  noise arises from the dominance of opposite-spin correlations— $\Delta_T^{\uparrow\downarrow}$  and  $\Delta_T^{\downarrow\uparrow}$ —which are significantly enhanced by spin-flip scattering in conjunction with Andreev reflection. As will be analyzed in detail in Sec. IV, this contribution dominates the same-spin contribution making the net spin  $\Delta_T$  noise negative.

A qualitative change emerges as temperature increases. At higher  $\frac{T}{T_C}$ , thermally activated quasiparticle transport channels at energies above the superconducting gap become prominent. These channels significantly enhance same-spin correlations,  $\Delta_T^{\uparrow\uparrow}$  and  $\Delta_T^{\downarrow\downarrow}$ , particularly via quasiparticle tunneling from the normal metal into the superconductor. Once these same-spin correlations dominate the opposite-spin correlations, the net spin  $\Delta_T$  noise,  $\Delta_T^{sp} = 2(\Delta_T^{\uparrow\uparrow} - \Delta_T^{\downarrow\downarrow})$ , undergoes a sign change from negative to positive. This sign change is clearly demonstrated in Fig. 3(b), where  $\Delta_T^{sp}$  transitions from negative at low  $\frac{T}{T_C}$  to positive at higher  $\frac{T}{T_C}$  in some particular values of  $J$  and  $Z$ . As can be seen in Fig. 3(b),  $\Delta_T^{sp}$  is completely negative in the regime  $1 \leq |J| \leq 3$ ,  $0 \leq Z \leq 0.5$  and  $0.1 \leq \frac{T}{T_C} \leq 0.5$ . The effect underscores the critical role of barrier strengths  $J$  and  $Z$  in tuning the qualitative behavior of spin  $\Delta_T$  noise.

#### B. Charge & spin quantum shot noise

To study the behavior of the charge as well as spin components of quantum shot noise, denoted by  $Q_{11}^{ch}$  and  $Q_{11}^{sp}$ , respectively, we focus on a finite voltage bias configuration applied across the junction. Specifically, we set the voltage biases of the two leads to  $V_1 = V$  and  $V_2 = 0$ , while keeping the temperatures identical on both sides,  $T_1 = T_2 = T$ . Figure 4(a) shows the charge quantum shot noise  $Q_{11}^{ch}$  as a function of  $J$ ,  $Z$ , and  $\frac{T}{T_C}$ . Our results reveal that  $Q_{11}^{ch}$  remains strictly positive over the entire parameter space, even when quasiparticle transport channels and spin-dependent scattering mechanisms are prominent. This robustness indicates that charge quantum shot noise is insensitive to potential sign reversals under voltage bias.

Turning to the spin component,  $Q_{11}^{sp}$ , we present the corresponding results in Fig. 4(b). Here, we observe that  $Q_{11}^{sp}$  also remains strictly positive for all values of  $J$ ,  $Z$ , and  $\frac{T}{T_C}$ , exhibiting a qualitative similarity to the charge quantum shot noise. This is in marked contrast to the spin  $\Delta_T$  noise,  $\Delta_T^{sp}$ , which, under temperature bias only, can become negative at low  $\frac{T}{T_C}$  due to the combined effects of spin-flip scattering and Andreev reflection. The key distinction lies in the nature of the driving mechanism:  $\Delta_T^{sp}$  originates from a purely thermal bias at zero voltage bias, the temperature gradients lead to non-equilibrium spin-current fluctuations, where spin-flip scattering and particle-hole conversion at the superconductor interface generates strong opposite-spin correlations, leading to spin  $\Delta_T$  noise being negative. In contrast,  $Q_{11}^{sp}$  is calculated at finite voltage bias. The observed positive  $Q_{11}^{sp}$  across the entire parameter space, even for large spin-flip strengths, implies that  $Q_{11}^{sp,sh}$  is dominated by the same spin correlations. This serves as a clear distinction between  $\Delta_T$  noise and quantum shot noise.

### IV. ANALYSIS

In this section, we present a detailed analysis of our results, focusing on the behavior of  $\Delta_T$  noise as a function of tempera-

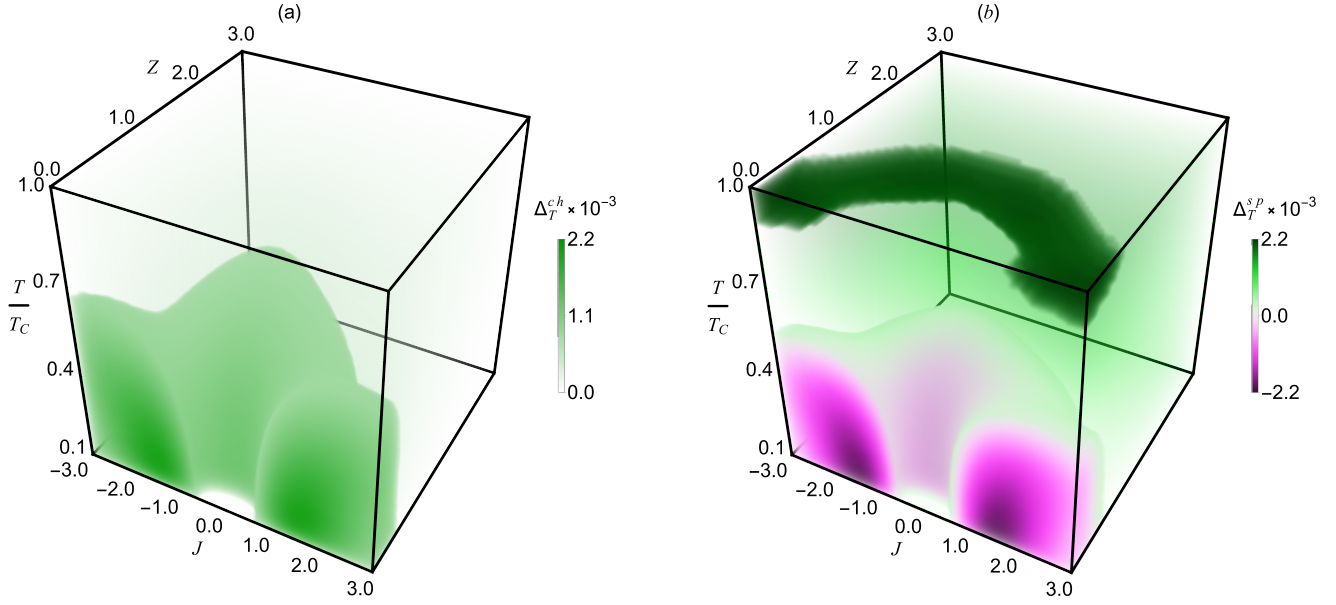


Figure 3: (a) Charge  $\Delta_T$  and (b) Spin  $\Delta_T$  noise. Parameters taken are  $\Delta T = 0.1T$ ,  $E_F = 100\Delta_0$  and  $\Delta_0 = 1.76k_B T_C$  with  $T_C = 18K$ .

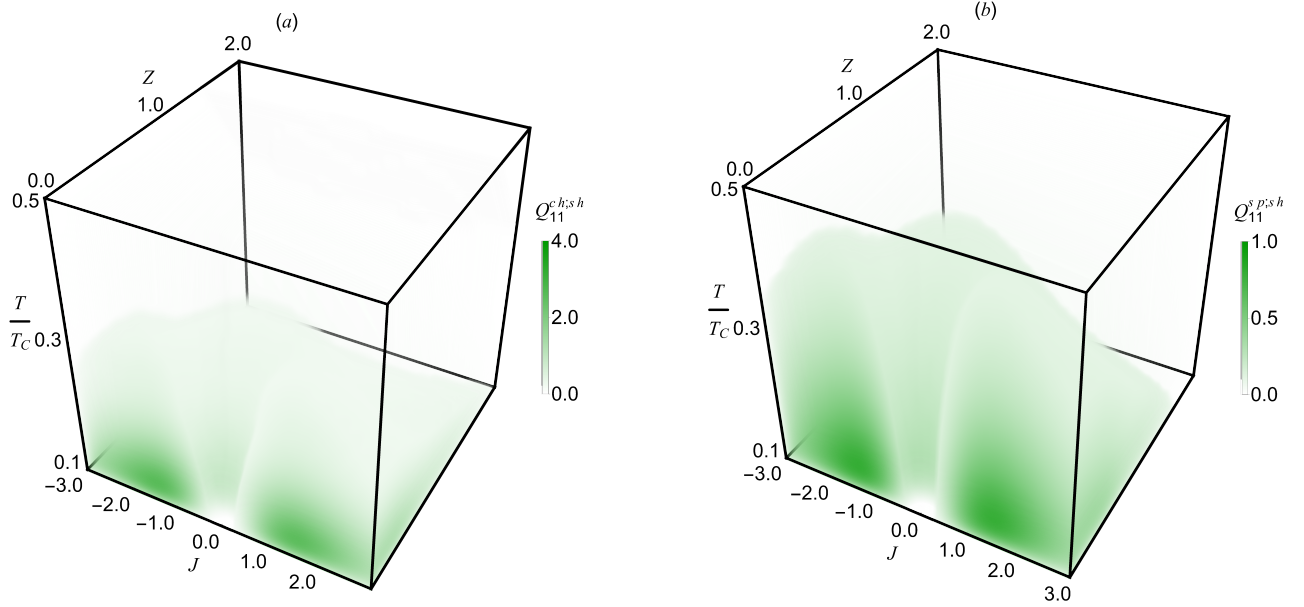


Figure 4: (a) Charge quantum shot noise and (b) Spin quantum shot noise. Parameters taken are  $\Delta T = 0.1T$ ,  $eV = 0.30\Delta_0$ ,  $E_F = 100\Delta_0$  and  $\Delta_0 = 1.76k_B T_C$  with  $T_C = 18K$ .

ture bias  $\Delta T/T$ , followed by a comparison with Refs. [2, 9, 11].

In Fig. 5(a), we plot  $\Delta_T^{ch}$  and  $\Delta_T^{sp}$  as a function of temperature bias  $\frac{\Delta T}{T}$  for  $J = 1.7$  for  $Z = 0$ ,  $Z = 1$  and  $Z = 3$ . In Table I, we summarize all our findings. We observe that both  $\Delta_T^{ch}$  and  $\Delta_T^{sp}$  are quadratic with  $\frac{\Delta T}{T}$ . For all the  $Z$  values,  $\Delta_T^{ch}$  is positive. However,  $\Delta_T^{sp}$  is always negative for  $s$ -wave. The sign of the spin  $\Delta_T$  noise is governed by the relative magni-

tudes of the spin-resolved noise correlators  $\Delta_T^{\uparrow\uparrow}$ ,  $\Delta_T^{\uparrow\downarrow}$ ,  $\Delta_T^{\downarrow\uparrow}$ , and  $\Delta_T^{\downarrow\downarrow}$ . These correlators arise from various transport processes, including quasiparticle transmission, Andreev reflection, and normal reflection. The total charge noise is given by

$$\Delta_T^{ch} = \Delta_T^{\uparrow\uparrow} + \Delta_T^{\uparrow\downarrow} + \Delta_T^{\downarrow\uparrow} + \Delta_T^{\downarrow\downarrow},$$

whereas the total spin noise is expressed as

$$\Delta_T^{\text{sp}} = \Delta_T^{\uparrow\uparrow} - \Delta_T^{\uparrow\downarrow} - \Delta_T^{\downarrow\uparrow} + \Delta_T^{\downarrow\downarrow}.$$

A sign reversal in  $\Delta_T^{\text{sp}}$  can occur when the cross-spin contributions  $\Delta_T^{\uparrow\downarrow}$  and  $\Delta_T^{\downarrow\uparrow}$  dominate over the same-spin terms  $\Delta_T^{\uparrow\uparrow}$  and  $\Delta_T^{\downarrow\downarrow}$ . In contrast, the charge noise  $\Delta_T^{\text{ch}}$  remains positive in such a scenario.

As shown in Eq. (17), we have the symmetry relations:  $\Delta_T^{\uparrow\uparrow} = \Delta_T^{\downarrow\downarrow}$  and  $\Delta_T^{\uparrow\downarrow} = \Delta_T^{\downarrow\uparrow}$ . This simplifies the expressions as

$$\Delta_T^{\text{ch}} = 2(\Delta_T^{\uparrow\uparrow} + \Delta_T^{\uparrow\downarrow}), \quad \Delta_T^{\text{sp}} = 2(\Delta_T^{\uparrow\uparrow} - \Delta_T^{\uparrow\downarrow}).$$

Thus,  $\Delta_T^{\text{sp}}$  can become negative when  $\Delta_T^{\uparrow\downarrow} > \Delta_T^{\uparrow\uparrow}$ . This condition is typically met when Andreev reflection and spin-flip scattering processes dominate over quasiparticle transmission, which we explain below.

In particular, as evident from Eq. (17), the expression for  $\Delta_T^{\uparrow\downarrow}$  contains a term of the form:

$$4\kappa^2 \left( \text{Re}(c_{\uparrow\uparrow}^S c_{\downarrow\uparrow}^{S*}) + \text{Re}(d_{\uparrow\uparrow}^S d_{\downarrow\uparrow}^{S*}) \right) \left( \text{Re}(b_{\uparrow\uparrow} b_{\downarrow\uparrow}^*) + \text{Re}(a_{\uparrow\uparrow} a_{\downarrow\uparrow}^*) \right) + 4\mathcal{R}_{\uparrow\uparrow}^A \mathcal{R}_{\downarrow\uparrow} + 4\mathcal{R}_{\downarrow\uparrow}^A \mathcal{R}_{\uparrow\uparrow} - 8\text{Re}(b_{\downarrow\uparrow} a_{\uparrow\uparrow}^* a_{\downarrow\uparrow} b_{\uparrow\uparrow}^*). \quad (19)$$

At low temperatures ( $\frac{T}{T_c} \lesssim 0.50$ ), the thermal excitation energy is much smaller than the superconducting gap, and only subgap excitations contribute to transport. In this regime, quasiparticle transmission between the normal metal and the superconductor is strongly suppressed, leading to vanishing quasiparticle transmission probabilities  $\mathcal{C}_S$  and  $\mathcal{D}_S$ , as well as  $|u|^2 - |v|^2 \rightarrow 0$ . Consequently, the same-spin correlators  $\Delta_T^{\uparrow\uparrow}$  and  $\Delta_T^{\downarrow\downarrow}$ , which contain the factor  $(\mathcal{R}^A + \mathcal{R})(\mathcal{C}^S + \mathcal{D}^S)$ , vanish identically. In contrast, the opposite-spin correlator  $\Delta_T^{\uparrow\downarrow}$  (and equivalently  $\Delta_T^{\downarrow\uparrow}$ ) reduces to the form  $\Delta_T^{\uparrow\downarrow} = 4\mathcal{R}_{\uparrow\uparrow}^A \mathcal{R}_{\downarrow\uparrow} + 4\mathcal{R}_{\downarrow\uparrow}^A \mathcal{R}_{\uparrow\uparrow} - 8\text{Re}(b_{\downarrow\uparrow} a_{\uparrow\uparrow}^* a_{\downarrow\uparrow} b_{\uparrow\uparrow}^*)$ . Here,  $\Delta_T^{\uparrow\downarrow}$  can be finite even when  $\Delta_T^{\uparrow\uparrow}$  is strictly zero. For the spin  $\Delta_T$  noise, defined as  $\Delta_T^{\text{sp}} = 2(\Delta_T^{\uparrow\uparrow} - \Delta_T^{\uparrow\downarrow})$ , to become negative in this low-temperature regime, it is necessary for  $\Delta_T^{\uparrow\downarrow}$  to be positive, which in turn requires  $4\mathcal{R}_{\uparrow\uparrow}^A \mathcal{R}_{\downarrow\uparrow} + 4\mathcal{R}_{\downarrow\uparrow}^A \mathcal{R}_{\uparrow\uparrow} > 8\text{Re}(b_{\downarrow\uparrow} a_{\uparrow\uparrow}^* a_{\downarrow\uparrow} b_{\uparrow\uparrow}^*)$ . As the temperature increases, quasiparticle transmission channels above the gap begin to activate. These channels gradually dominate over both Andreev reflection and spin-flip scattering, thereby enhancing the same-spin contributions  $\Delta_T^{\uparrow\uparrow}$  relative to the opposite-spin terms  $\Delta_T^{\uparrow\downarrow}$ . Eventually, when  $\Delta_T^{\uparrow\uparrow} > \Delta_T^{\uparrow\downarrow}$ ,  $\Delta_T^{\text{sp}}$  switches sign from negative to positive.

The negative prefactor in the above expression, derived solely from Andreev and spin-flip scattering, plays a pivotal role in determining the sign of the spin-resolved  $\Delta_T$  noise. This highlights the importance of the interplay between these scattering processes.

To further illustrate this point, we plot in Fig. 5(b) the individual contributions  $\Delta_T^{\uparrow\uparrow}$  (equivalent to  $\Delta_T^{\downarrow\downarrow}$ ) and  $\Delta_T^{\uparrow\downarrow}$  (equivalent to  $\Delta_T^{\downarrow\uparrow}$ ). It is clearly observed that  $\Delta_T^{\uparrow\downarrow}$  exceeds  $\Delta_T^{\uparrow\uparrow}$ , leading to negative spin  $\Delta_T$  noise  $\Delta_T^{\text{sp}}$ . The underlying expression

incorporates all relevant spin-flip and Andreev scattering contributions, emphasizing their critical role in shaping the spin-resolved noise characteristics.

### A. Why the sign change does not occur in spin quantum shot noise

Turning now to the quantum shot noise, we realize that the  $Q_{11}^{\text{ch}}$  remains positive irrespective of any regime. More interestingly,  $Q_{11}^{\text{sp}}$  also remains positive, even though  $\Delta_T^{\text{sp}}$  was negative in that regime. This key observation can be understood by analyzing the structure of the shot noise expression (see, Eq. (16)), which includes two types of contributions: one proportional to  $(f_{1e} - f_{2e})^2$  and another to  $(f_{1e} - f_{1h})^2$ . In regimes with finite spin current and voltage bias, the latter term can dominate, resulting in a positive  $Q_{11}^{\text{sp}}$  even if the  $(f_{1e} - f_{2e})^2$  term would predict a negative contribution. Even in the low-temperature regime, when the condition  $4\mathcal{R}_{\uparrow\uparrow}^A \mathcal{R}_{\downarrow\uparrow} + 4\mathcal{R}_{\downarrow\uparrow}^A \mathcal{R}_{\uparrow\uparrow} > 8\text{Re}(b_{\downarrow\uparrow} a_{\uparrow\uparrow}^* a_{\downarrow\uparrow} b_{\uparrow\uparrow}^*)$  is satisfied, the additional contribution  $(2\mathcal{R}^A \mathcal{R} - 8\text{Re}(a_{\uparrow\uparrow} a_{\downarrow\uparrow}^*) \text{Re}(r_N^{\uparrow\uparrow} b_{\downarrow\uparrow}^*))$ , which serves as the coefficient of  $(f_{1e} - f_{1h})^2$ , remains finite and in fact dominates over the coefficient of  $(f_{1e} - f_{2e})^2$  even at low temperatures. As a result, the spin quantum shot noise remains positive regardless of the parameter regime. This distinction between spin  $\Delta_T$  noise and spin quantum shot noise highlights the fundamentally different roles played by thermal and shot noise in probing spin-dependent transport.

To our knowledge, this is the first study that establishes a clear and qualitative distinction between  $\Delta_T$  noise and quantum shot noise.

### B. Comparison with existing literature

In Ref. [2], it was demonstrated that the charge  $\Delta_T$  noise can undergo a sign reversal in a two-terminal mesoscopic setup involving a quantum point contact within the fractional quantum Hall (FQH) regime. This intriguing behavior stems from the tunneling of Laughlin quasiparticles, whose fractional statistics and anyonic nature lead to noise characteristics that are fundamentally different from those arising from conventional electron tunneling. Notably, such sign changes in the charge  $\Delta_T$  noise are not achievable with ordinary electron tunneling.

In a complementary direction, Ref. [11] investigates the relation between sign of  $\Delta_T$  noise and the exchange statistics of the tunneling quasiparticles in one-dimensional interacting systems. The central result of that work is that the sign of the  $\Delta_T$  noise is generally governed by the dominant tunneling process, which is characterized by the scaling dimension of the leading tunneling operator. Specifically, the study shows that in interacting chiral systems, negative  $\Delta_T$  noise is often associated with boson-like quasiparticles that tend to bunch—though the reverse is not necessarily true. However, in this work we demonstrate that when the opposite-spin correlations, such as  $\Delta_T^{\uparrow\downarrow}$  and  $\Delta_T^{\downarrow\uparrow}$ , dominate over the same-spin correlations  $\Delta_T^{\uparrow\uparrow}$  and

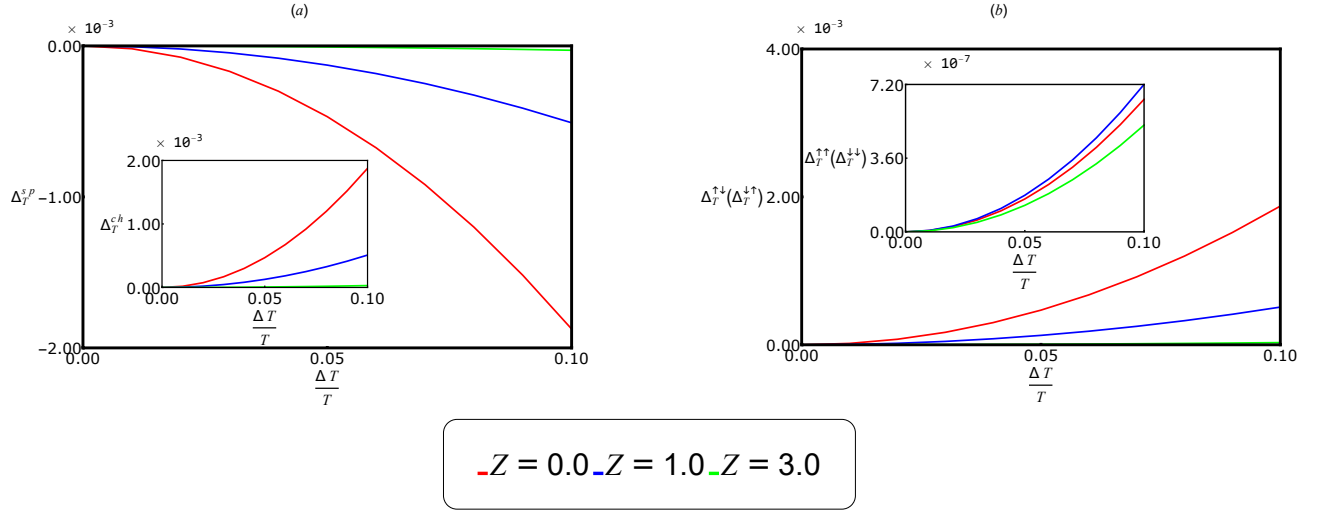


Figure 5: (a) Spin  $\Delta_T$  noise (Charge  $\Delta_T$  noise in the inset), (b)  $\Delta_T^{\uparrow\downarrow}(\Delta_T^{\downarrow\uparrow})$  ( $\Delta_T^{\uparrow\uparrow}(\Delta_T^{\downarrow\downarrow})$ ). The parameters taken are  $J = 1.7$ ,  $\frac{T}{T_C} = 0.28$ ,  $E_F = 100\Delta_0$  and  $\Delta_0 = 1.76k_B T_C$  with  $T_C = 18K$ .

Table I: Sign of charge/spin  $\Delta_T$  noise and charge/spin quantum shot noise

	$\frac{T}{T_C} \lesssim 0.50$			$\frac{T}{T_C} \gtrsim 0.50$		
	$J < 0$		$J > 0$	$J < 0$		$J > 0$
	$Z = 0$	$Z = 1$	$Z = 3$	$Z = 0$	$Z = 1$	$Z = 3$
	$Z = 0$	$Z = 1$	$Z = 3$	$Z = 0$	$Z = 1$	$Z = 3$
$\Delta_T^{ch}$	Positive	Positive	Positive	Positive	Positive	Positive
$\Delta_T^{sp}$	Negative	Negative	Negative	Positive	Positive	Positive
$Q_{11}^{ch;sh}$	Positive	Positive	Positive	Zero	Zero	Zero
$Q_{11}^{sp;sh}$	Positive	Positive	Positive	Zero	Zero	Zero

Table II: Comparison of sign reversal mechanisms of  $\Delta_T$  noise in various mesoscopic systems

Work	Physical Mechanism	Sign Behavior of $\Delta_T$ Noise	Experimental Realization	Application
<b>Negative <math>\Delta_T</math> noise in the fractional quantum Hall effect; Ref. [2]</b>	Tunneling of Laughlin quasiparticles in fractional quantum Hall (FQH) regime via QPC	Sign change in <i>charge</i> $\Delta_T$ noise due to fractional statistics	Requires FQH setup and precise QPC engineering	Probing fractional statistics and anyonic quasiparticles
<b><math>\Delta_T</math> noise for weak tunneling in one-dimensional systems: Interactions versus quantum statistics; Ref. [11]</b>	Dominant tunneling operator characterized by scaling dimension; statistics of quasiparticles in 1D chiral systems	Sign depends on quasiparticle statistics; negative $\Delta_T$ noise often linked to bosonic bunching	Needs controlled 1D interacting systems with chiral edge modes, but with fractional filling factor	Exploring interaction and statistics effects in low-dimensional systems
<b>This work</b>	Quasiparticles with integer charge undergoing spin-flip scattering and Andreev reflection at finite temperature in N-sf-N-I-S junction	Sign reversal in spin $\Delta_T$ noise without any Laughlin-type quasiparticles and edge mode transport	Fully realizable with conventional metals, magnetic impurities, and superconductors	Detecting spin-dependent noise signatures and first phenomenon where spin $\Delta_T$ noise shows completely opposite behavior to spin quantum shot noise.

$\Delta_T^{\downarrow\downarrow}$ , the spin  $\Delta_T$  noise becomes negative. This situation arises at low temperatures, where quasiparticle transmission from the normal metal into the superconductor is strongly suppressed. In contrast, for the spin quantum shot noise, even at low tem-

peratures, the same-spin correlations  $Q_{11}^{sh;\uparrow\uparrow}$  and  $Q_{11}^{sh;\downarrow\downarrow}$  remain dominant over the opposite-spin correlations  $Q_{11}^{sh;\uparrow\downarrow}$  and  $Q_{11}^{sh;\downarrow\uparrow}$ . As a result, the spin quantum shot noise stays strictly positive,



in contrast to spin  $\Delta_T$  noise.

More recently, Ref. [9] explores cross-correlated  $\Delta_T$  noise in a multiterminal hybrid junction involving superconductors and edge states of the integer quantum Hall (IQH) effect. The study reveals that, under zero voltage bias and finite temperature gradient, the sign of the cross-correlated  $\Delta_T$  noise can transition from negative to positive, due to the complex interplay between scattering at the edge, Andreev reflection, and proximity-induced coherence. However, in the absence of Andreev reflection, the cross-correlated  $\Delta_T$  noise remains strictly negative. However, in principle, shot noise cross-correlation can change sign in presence of complicated scattering processes involving Andreev reflection and there is nothing new in this case as this has been shown in many Refs. including [23–25] in quantum Hall setup as well as superconducting junctions.

In contrast to these previous studies, our work shows that a sign change in the spin  $\Delta_T$  noise can occur even in the absence of edge mode transport, whether its due to fractional quantum Hall effect or interger quantum Hall effect. Specifically, we demonstrate that subject to spin-flip scattering, Andreev reflection, and finite temperature, is sufficient to induce a sign reversal in the spin  $\Delta_T$  noise.

We have put a comparison of the physical mechanisms, sign behavior of  $\Delta_T$  noise, as well as applications of  $\Delta_T$  noise of all the Refs. [2, 11] and our work in Table II. This reveals that rich spin-dependent transport phenomena and nontrivial  $\Delta_T$  noise behavior emerge in topologically trivial systems, thereby broadening the scope of mesoscopic noise-based probes of many-body physics and quasiparticle dynamics in hybrid structures.

## V. EXPERIMENTAL REALIZATION AND CONCLUSION

In this work, we investigate charge (spin)  $\Delta_T$  noise in the N-sf-N-I-S junction operating in the quantum ballistic transport regime. Our analysis uncovers key insights into the interplay between spin-flip scattering, Andreev reflection, and ther-

mal transport in these hybrid systems. Importantly, the magnetic impurity and insulating barrier components proposed can be readily realized in experiments, rendering our setup both experimentally accessible and technologically relevant. We observe a notable sign reversal in the spin  $\Delta_T$  noise, with negative values emerging from the combined influence of spin-flip scattering—modeled as an Anderson-type spin flipper at the magnetic impurity site—and Andreev reflection at the superconductor interface. These results compellingly illustrate how superconducting correlations and spin dynamics intertwine to shape thermally driven noise characteristics.

Furthermore, our results reveal a fundamental distinction between spin  $\Delta_T$  noise versus spin quantum shot noise. While spin  $\Delta_T$  noise can change sign—becoming negative depending on temperature and scattering strength—spin quantum shot noise remains strictly positive across all regimes. Specifically, variations in temperature can induce sign changes in spin  $\Delta_T$  noise, whereas spin quantum shot noise never exhibits such sign reversals. This contrast highlights the complementary nature of  $\Delta_T$  noise and quantum shot noise as probes of spin-dependent phenomena. Importantly, we report for the first time the occurrence of negative spin  $\Delta_T$  noise autocorrelation driven by the interplay of spin-flip scattering and Andreev reflection in the ballistic transport regime. Previous studies have documented negative charge  $\Delta_T$  noise autocorrelations in fractional quantum Hall systems with quantum point contacts [2, 11]. In contrast, our findings demonstrate that this effect can be realized without relying on edge-mode transport, instead arising from the presence of a magnetic impurity inducing spin-flip scattering combined with Andreev reflection.

From an experimental perspective, our study is closely aligned with recent advancements in measuring temperature-gradient-driven noise in mesoscopic conductors [4, 6]. Our theoretical framework provides a concrete proposal to observe the sign reversal of spin  $\Delta_T$  noise in 2DEG-based junctions, where engineered magnetic impurities or quantum dots function as spin flippers. In summary, this work demonstrates that even in conventional ballistic junctions, the spin  $\Delta_T$  noise can undergo a sign reversal, highlighting the rich interplay between spin dynamics and thermal transport.

- 
- [1] J. Eriksson, M. Acciai, L. Tesser, and J. Splettstoesser, General bounds on electronic shot noise in the absence of currents, *Phys. Rev. Lett.* **127**, 136801 (2021).
  - [2] J. Rech, T. Jonckheere, B. Grémaud, and T. Martin, Negative Delta- $T$  noise in the Fractional Quantum Hall Effect, *Phys. Rev. Lett.* **125**, 086801 (2020).
  - [3] A. Popoff, J. Rech, T. Jonckheere, L. Raymond, B. Grémaud, S. Malherbe, and T. Martin, Scattering theory of non-equilibrium noise and delta  $T$  current fluctuations through a quantum dot, *Journal of Physics: Condensed Matter* **34**, 185301 (2022).
  - [4] O. S. Lumbroso, L. Simine, A. Nitzan, D. Segal, and O. Tal, Electronic noise due to temperature differences in atomic-scale junctions, *Nature* **562**, 240 (2018).
  - [5] O. Shein-Lumbroso, Electronic noise in atomic and molecular junctions: Beyond the known noise contributions, *PhD Thesis* Weizmann Institute of Science (2022).
  - [6] E. Sivre, H. Duprez, A. Anthore, A. Aassime, F. Parmentier, A. Cavanna, A. Ouerghi, U. Gennser, and F. Pierre, Electronic heat flow and thermal shot noise in quantum circuits, *Nature Communications* **10**, 5638 (2019).
  - [7] L. Tesser, M. Acciai, C. Spaanslatt, J. Monsel, and J. Splettstoesser, Charge, spin, and heat shot noises in the absence of average currents: Conditions on bounds at zero and finite frequencies, *Phys. Rev. B* **107**, 075409 (2023).
  - [8] S. Mishra, A. R. Dora, T. Mohapatra, and C. Benjamin, *Andreev reflection mediated  $\Delta_T$  noise* (2024), [arXiv:2403.10990](https://arxiv.org/abs/2403.10990) [cond-mat.mes-hall].
  - [9] L. Pierattelli, F. Taddei, and A. Braggio,  $\Delta T$ -noise in multiterminal hybrid systems, *Phys. Rev. Res.* **7**, 023321 (2025).
  - [10] S. Mishra and C. Benjamin, Probing the dichotomy between Yu-Shiba-Rusinov and Majorana bound states via conductance, quantum noise, and  $\Delta_T$  noise, *Phys. Rev. B* **112**, 024505 (2025).

- [11] G. Zhang, I. V. Gornyi, and C. Spaanslatt, Delta- $T$  noise for weak tunneling in one-dimensional systems: Interactions versus quantum statistics, *Phys. Rev. B* **105**, 195423 (2022).
- [12] The Mathematica codes are available: <https://github.com/Sachiraj/Charge-Spin-Delta-T.git>.
- [13] T. Mohapatra, S. Pal, and C. Benjamin, Probing the topological character of superconductors via nonlocal Hanbury Brown and Twiss correlations, *Phys. Rev. B* **106**, 125402 (2022).
- [14] C.-K. Chiu, J. C. Y. Teo, A. P. Schnyder, and S. Ryu, Classification of topological quantum matter with symmetries, *Rev. Mod. Phys.* **88**, 035005 (2016).
- [15] A. P. Schnyder, S. Ryu, A. Furusaki, and A. W. W. Ludwig, Classification of topological insulators and superconductors in three spatial dimensions, *Phys. Rev. B* **78**, 195125 (2008).
- [16] B. T. Matthias, T. H. Geballe, S. Geller, and E. Corenzwit, Superconductivity of  $\text{Nb}_3\text{Sn}$ , *Phys. Rev.* **95**, 1435 (1954).
- [17] Z. Sun, Z. Baraissov, R. D. Porter, L. Shpani, Y.-T. Shao, T. Osleroff, M. O. Thompson, D. A. Muller, and M. U. Liepe, Smooth, homogeneous, high-purity  $\text{Nb}_3\text{Sn}$  superconducting RF resonant cavity by seed-free electrochemical synthesis, *Superconductor Science and Technology* **36**, 115003 (2023).
- [18] O. L. T. de Menezes and J. S. Helman, Spin flip enhancement at resonant transmission, *Am. J. Phys* **53**, 1100 (1985).
- [19] S. Pal and C. Benjamin, Spin-flip scattering engendered quantum spin torque in a Josephson junction, *Proceedings of the Royal Society A* **475**, 20180775 (2019).
- [20] S. Pal and C. Benjamin, Yu-Shiba-Rusinov bound states induced by a spin flipper in the vicinity of a  $s$ -wave superconductor, *Scientific reports* **8**, 11949 (2018).
- [21] M. P. Anantram and S. Datta, Current fluctuations in mesoscopic systems with andreev scattering, *Phys. Rev. B* **53**, 16390 (1996).
- [22] Y. M. Blanter and M. Büttiker, Shot noise in mesoscopic conductors, *Phys. Rep.* **336**, 1 (2000).
- [23] C. Texier and M. Büttiker, Effect of incoherent scattering on shot noise correlations in the quantum hall regime, *Phys. Rev. B* **62**, 7454 (2000).
- [24] C. Benjamin and J. K. Pachos, Detecting entangled states in graphene via crossed Andreev reflection, *Phys. Rev. B* **78**, 235403 (2008).
- [25] A. Mani and C. Benjamin, Probing helicity and the topological origins of helicity via non-local Hanbury-Brown and Twiss correlations, *Sci. Rep.* **7**, 6954 (2017).